Analysis and Simulation of the P&O MPPT Algorithm Using a Linearized PV Array Model

Marcelo G. Villalva, Ernesto Ruppert F.

School of Electrical and Computer Engineering
University of Campinas – UNICAMP, Brazil
Email: mvillalva@gmail.com, ruppert@fee.unicamp.br

***Abstract*—This paper shows that the performance of the perturb and observe (P&O) maximum power point tracking (MPPT) algorithm is improved when the electronic converter is correctly controlled. A linearized photovoltaic (PV) array model is used to obtain the transfer function of the electronic converter and to design a voltage compensator for the converter input voltage. A buck converter is used in this work.**

***Keywords* – maximum power point, MPPT, PV, photovoltaic, perturb, observe.**

I. Introduction

A photovoltaic (PV) array converts sunlight into electricity. The voltage and current available at the terminals of the PV array may directly feed small loads such as lighting systems and DC motors. More sophisticated applications require electronic converters to process the electricity from the array. These converters may be used to regulate the voltage and current at the load, to control the power flow in grid-connected systems and mainly to track the maximum power point (MPP) of the array.

Converters with the maximum power point tracking (MPPT) feature use an algorithm to continuously detect the maximum instantaneous power of the PV array. Because the operating conditions of the array (solar irradiation and temperature) may change randomly during the operation of the system an MPPT algorithm is necessary so that the maximum instantaneous power can be extracted and delivered to the load.

Many MPPT altorithms have been proposed in the literature. A quick search in the IEEExplore database returns hundreds of publications on this subject. Many theoretical improvements and even advanced techniques of artificial intelligence have been proposed to enhance a few basic MPPT methods in order to obtain questionable performance improvements. In [1] a review of the basic MPPT methods is presented. The simplest MPPT method analyzed in [1] is the perturb and observe (P&O) method. This method appeared in works such as [2], [3] and has been further investigated in [4–9].

II. MPPT and the P&O method

Fig. 1 shows the figure of a PV system where a PV array feeds a DC-DC converter. The output of the converter is represented by a constant DC voltage source. This kind of converter with constant output voltage may be used in battery charging systems or in systems with a second cascaded conversion stage (e.g. DC-AC). The output power of the PV array is regulated by the converter. In this example the MPPT block observes the power at the terminals of the array and controls the input voltage or the input current of the converter, forcing the PV array to operate at the maximum power point.

Depending on the converter topology one may choose the voltage or current as the control variable. Fig. 2 shows a buck converter whose input voltage is controlled [2], [3]. Because the input current of the buck converter is discontinuous and the capacitor provides a low voltage ripple, the MPPT algorithm can be used to control the output voltage of the PV array. The output capacitor C is necessary to keep the array output voltage constant and to filter the discontinuity of the buck input current. Of course one can chose to measure the output current of the PV array before the capacitor and use the current as the control variable. Yet another possibility is to control the output current of the buck converter and observe the output power of the converter instead of observing the output power of the PV array. If a boost converter is employed, as shown in Fig. 3, the output current of the PV array and the converter inductor current are the same, so the MPPT algorithm can observe the array output power and optionally use the converter inductor current as the control variable [6], [7], [10].

Many configurations and control schemes are possible and each one presents pros and cons. If the MPPT algorithm observes the converter output power the global efficiency of the system (including the PV array and the converter) [1] is considered and the system output power is optimized. If the MPPT observes the array output power only the PV

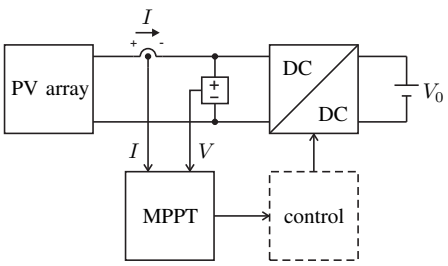

Figure 1. PV array feeding a DC-DC converter with constant output voltage. The MPPT block observes the array output power and controls the converter current or voltage.

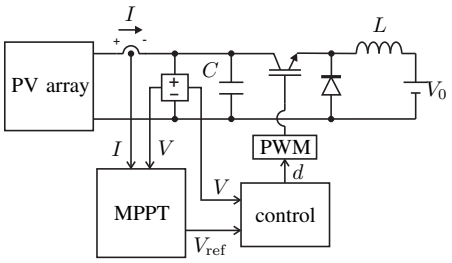

Figure 2. PV system with buck converter. The MPPT block determines the reference of the input voltage of the converter. The voltage controller controls the duty-cycle of the converter switch. The capacitor filters the AC component of the discontinuous input current of the converter.

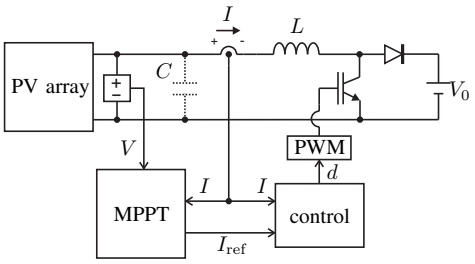

Figure 3. PV system with boost converter. The MPPT block determines the reference of the input current of the converter. The current controller controls the duty-cycle of the converter switch. The optional input capacitor reduces the voltage ripple.

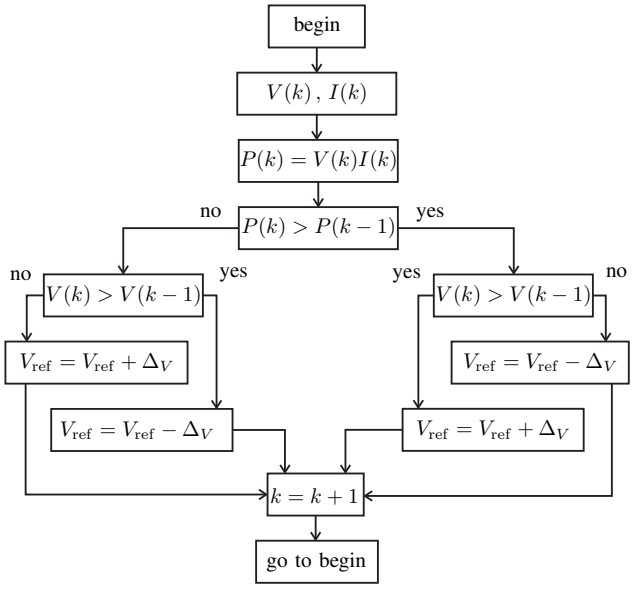

Figure 4. Algorithm of the P&O method.

array power is optimized and the converter efficiency is not taken into account. Because converter efficiencies for PV applications are generally very high, in practice there is little or no difference on the system performance depending on the MPPT configuration employed.

Fig. 4 shows the algorithm of the P&O MPPT method. As the name says, the algorithm is based on the observation of the array output power and on the perturbation of the power based on increments of the array voltage or current. The algorithm continuously increments or decrements the reference current or voltage based on the value of the previous power sample.

The P&O method is claimed to have slow dynamic response and high steady state error [1]. In fact, the dynamic response is low when a small increment value and a low sampling rate are employed. Low increments are necessary to decrease the steady state error because the P&O always makes the operating point oscillate near the MPP, but never at the MPP exactly. The lower the increment, the closer the system will be to the array MPP. The greater the increment, the faster the algorithm will work, but the steady state error will be increased. Considering that a low increment is necessary to achieve a satisfactory steady state error, the algorithm speed may be increased with a higher sampling rate. So there is always a compromise between the increment and the sampling rate in the P&O method.

In [7] there is a discussion about the effects of the size of the increment on the performance of the P&O method. The conclusion is that small increments tend to make the algorithm more stable and accurate when the operating conditions of the PV array change. Large increments tend to make the algorithm confused since the response of the converter to large voltage or current variations will cause oscillations, overshoot and the settling time of the converter itself confuses the algorithm. The theoretical analysis carried in [7], although it is correct and confirms the idea that small increments are better for the stability of the algorithm, is based on the direct duty-cycle control of the DC-DC converter. The direct duty-cycle control is employed in a great number of works related to DC-DC converters for PV applications. However, as stated in [11] in the early 1990, this kind of control is not recommended because the converter is subject to increased switching stress and losses. A feedback control with a proportional and integral (PI) compensator for the converter current or voltage is preferred. Besides reducing losses and stress due to the bandwidth-limited regulation of the duty-cycle, the presence of the controller reduces the settling time of the converter and avoids oscillation and overshoot, making easier the functioning of the P&O algorithm.

Another important consideration about the optimization of the P&O method is found in [6], where the authors analyze the effect of the sampling rate on the performance of the P&O method. It is suggested in [6] that the sampling rate of the P&O method must be chosen in accordance with the dynamic behavior of the converter. The analysis, although it leads to a valid and necessary conclusion, is carried with the duty-cycle controlled converter. In this kind of control, as discussed above, there are severe drawbacks. The idea of determining the optimized sampling rate in accordance with the settling time of the converter is correct, provided that the converter is controlled with some kind of feedback current or voltage control. A duty-cycle controlled converter is, in fact, an open-loop converter.

One should not expect the MPPT algorithm to control the

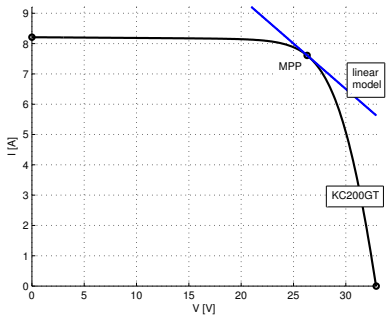

Figure 5. Nonlinear I-V characteristic of the KC200GT PV array and curve of the equivalent linear model at the MPP.

converter. The MPPT converter provides no feedback for the controlled variable (current or voltage). The MPPT algorithm feedbacks the power and based on an entirely nonlinear process provides a reference for the controlled variable. The agorithm should not be responsible for controlling this variable, as many authors have proposed. In 1998 the authors of [3] analyzed the P&O with the scheme of Fig. 2 using a PI compensator to control the converter input voltage according to the reference voltage determined by the algorithm. Curiously some years later the authors of [2] proposed a similar P&O method without the PI compensator and claimed this to be an improvement.

The conflict between the proposals of [2] and [3], considering the conclusions based on the analyzes of [6], [7] require a better evaluation of the P&O method. This paper proposes a P&O method working together with a voltage controller composed of a PI compensator and a PWM modulator. The analysis is done with the buck-based system of Fig. 2. The compensator is designed with knowledge of the dynamic characteristics of the converter. These characteristics are obtained from the linearized model of the PV array at the nominal operation point and of the buck converter considering that the input voltage of the converter is the controlled variable.

III. Modeling and Controlling the PV-Buck System

A. PV array

The PV array presents a nonlinear characteristic illustrated in Fig. 5. In this example the KC200GT [12] solar array is used. The dynamic behavior of the PV-buck system depends on the point of operation of the PV array. Because the array directly feeds the buck converter, it may not be neglected and must be considered in the dynamic model of the converter.

The equation of the I-V characteristic is given by [13]:

$$I = I_{\mathrm{pv}} - I_0 \left[\exp\left(\frac{V + R_{\mathrm{s}} I}{V_{\mathrm{t}} a} \right) - 1 \right] - \frac{V + R_{\mathrm{s}} I}{R_{\mathrm{p}}} \quad (1)$$

where I_{pv} and I_0 are the PV and saturation currents of the array, $V_{\mathrm{t}} = N_{\mathrm{s}} kT/q$ is the thermal voltage of the array with N_{s} cells connected in series, R_{s} is the equivalent series resistance of the array, R_{p} is the equivalent shunt resistance, and a is the ideality constant of the diode. The parameters of the PV array equation (1) may be obtained from measured or practical information obtained from the datasheet: open-circuit voltage, short-circuit current, maximum-power voltage, maximum-power current, and current/temperature and voltage/temperature coefficients. A complete explanation of the determination of the parameters of the I-V equation may be found in [13].

Table I
Parameters of the adjusted model of the KC200GT solar array at nominal operating conditions.

I_{mp}	7.61 A
V_{mp}	26.3 V
P_{max}	200.143 W
V_{oc}	32.9 V
$I_{0,n}$	$9.825 \cdot 10^{-8}$ A
I_{pv}	8.214 A
a	1.3
R_{p}	415.405 Ω
R_{s}	0.221 Ω

As the PV system is expected to work near the MPP, the I-V curve may be linearized at this point. The derivative of the I-V curve at the MPP is given by:

$$g(V_{\mathrm{mp}}, \mathrm{I_{mp}}) = -\frac{I_0}{V_{\mathrm{t}} N_{\mathrm{s}} a} \exp\left[\frac{V_{\mathrm{mp}} + \mathrm{I_{mp}} R_{\mathrm{s}}}{V_{\mathrm{t}} N_{\mathrm{s}}} \right] - \frac{1}{R_{\mathrm{p}}} \quad (2)$$

The PV array is modeled with the following linear equation at the MPP point:

$$I = (-g V_{\mathrm{mp}} + I_{\mathrm{mp}}) + gV \quad (3)$$

Fig. 5 shows the nonlinear I-V characteristic of the PV array superimposed with the linear I-V curve described by (3). The parameters of the I-V equation obtained with the modeling method proposed in [13] are listed in Table I. From these parameters, with (2) and (3), the equivalent voltage source and series resistance of the PV array linearized at the MPP are obtained: $V_{\mathrm{eq}} = 51.6480\,[\mathrm{V}]$ and $R_{\mathrm{eq}} = 3.3309\,[\Omega]$.

B. Buck converter

Fig. 6 shows the buck converter fed by the linear PV array model. This approximation is valid at the vicinities of the MPP point. Once the PV model has been linearized, the next step is to obtain a linear model of the entire PV-buck system. This subject was discussed in [14–16] with different modeling approaches and using a simplified PV array model. The buck converter may be modeled and linearized by the principe of average variables. First, the nonlinear switching elements (transistor and diode) are replaced by a theoretical DC transformer, as shown in Fig. 7. The DC transformer is described by (4), where the variables between the $<>$ symbols are the average values of the instantaneous voltages and currents of the converter in one switching period, and d is the duty-cycle of the converter in this period.

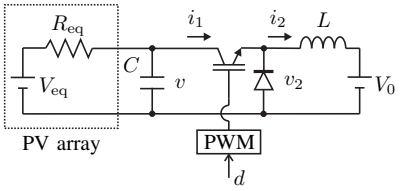

Figure 6. Buck converter fed by the linear PV array circuit model.

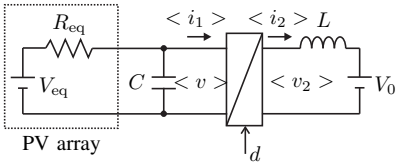

Figure 7. PV-buck system without the switching elements.

$$\begin{aligned} < v_2 > &= d < v > \\ < i_1 > &= d < i_2 > \end{aligned} \tag{4}$$

The circuit of Fig. 7 is simplified by decomposing the average variables in DC and small AC components according to (5) [14–16]. After the variables have been decomposed and the DC and nonlinear terms have been eliminated the small-signal linear AC circuit of Fig. 8 is obtained.

$$\begin{aligned} < v > &= V + \hat{v} \\ < v_2 > &= V_2 + \hat{v}_2 \\ < i_1 > &= I_1 + \hat{i}_1 \\ < i_2 > &= I_2 + \hat{i}_2 \\ d &= D + \hat{d} \end{aligned} \tag{5}$$

The small-signal transfer function of the PV-buck system is obtained from the circuit of Fig. 8 [14–16]:

$$G_{\mathrm{vd}}(s) = \frac{\widehat{v}}{\widehat{d}} = \frac{R_{\mathrm{eq}}(DV + sLI_2)}{s^2 LCR_{\mathrm{eq}} + sL + D^2 R_{\mathrm{eq}}} \tag{6}$$

where D is the steady-state duty-cycle of the converter and $V = V_0/D$ and $I_2 = (V_{\mathrm{eq}} - V)/(R_{\mathrm{eq}}D)$ are the steady-state values of v and i_2.

C. Compensator design

The uncompensated linearized PV-buck system with the parameters of Tables I and II presents the frequency-domain response (dashed line) seen in Fig. 9. Although the system is stable and has a good phase margin, it presents a very low DC gain and a low crossover frequency.

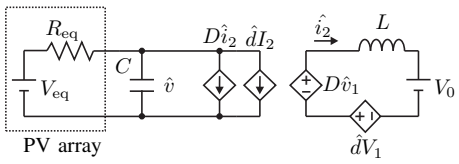

Figure 8. Linear small-signal PV-buck system.

Table II
PARAMETERS OF THE BUCK CONVERTER.

L	1 mH
C	1000 μF
V_0	13.15 V
D	0.5
I	15.22 A
V	26.30 V

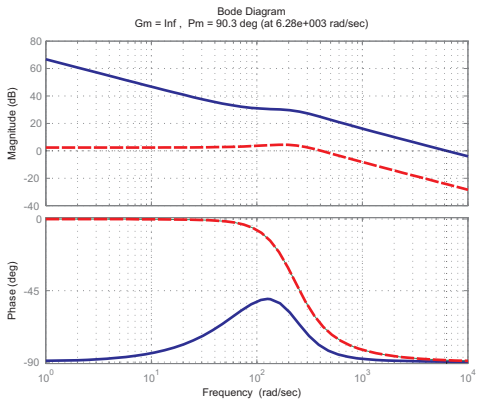

Figure 9. Frequency response of the uncompensated (dashed line) and of the compensated (continuous line) linearized PV-buck system.

The system response may be improved with a PI compensator designed to originate a feedback system with zero steady-state error and control bandwidth of 1 kHz. The compensated system, with feedback gain $H = 0.025$, presents the frequency response (continuous line) seen in Fig. 9. Any conventional control design method may be employed [14].

Fig. 10 shows the time-domain responses of the open-loop converter and of the converter controlled with the PI compensator. As expected, the input voltage of the uncontrolled converter presents oscilations, overshoot and high settling time. The controlled converter rapidly and accurately reaches the reference voltage, without any oscillation.

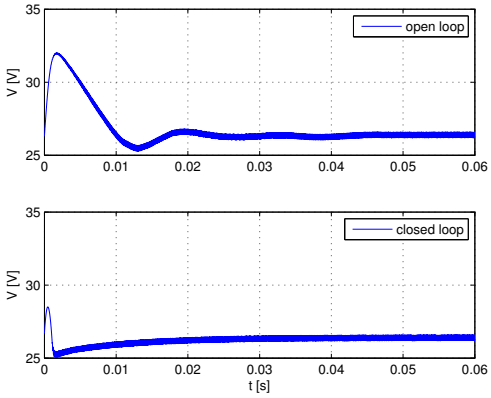

Figure 10. Open-loop (top) and closed-loop (bottom) time-domain responses of the converter.

IV. PV-BUCK SYSTEM WITH THE P&O MPPT ALGORITHM – SIMULATION RESULTS

The buck converter fed by the PV array illustrated in Fig. 2 was simulated and the results are plotted in Figs. 11-18. The simulations where carried with different conditions and the results permit to make comparisons and observe the effects of the parameters of the P&O algorithm and the effect of the voltage controller with PI compensator. The algorithm of Fig. 4 was used in the simulations and the PI compensator was designed to achieve the closed-loop response presented in Fig. 9. The compensator design was based on the system linear transfer function (6) developed in the previous section. In all simulations the PV array initially operates at the nominal conditions ($G = 1000\,\mathrm{W/m^2}$ and $T = 25°\mathrm{C}$), then at $t = 0.4\,\mathrm{s}$ the irradiation is suddenly reduced to $G = 500\,\mathrm{W/m^2}$ and at $t = 0.8\,\mathrm{s}$ the temperature is increased to $T = 75°\mathrm{C}$.

Figs. 11-14 show the results of the simulation employing the voltage controller with PI compensator. In this system the converter input voltage is controlled to follow the reference determined by the P&O algorithm. These figures show that the system behaves perfectly well when the voltage controller is employed. The system precisely tracks the maximum power and the input voltage of the algorithm has low ripple. As the voltage increment is fixed, the time response of the P&O method depends on the sampling time of the algorithm (T_s). As seen in the simulation results, the speed of the system is limited by the sampling time of the P&O algorithm and is not significantly influenced by the converter dynamics, since the voltage controller is sufficiently fast and accurate for this application.

Figs. 15-18 show the results of the simulation of the system without the voltage controller. Only the P&O algorithm and the converter are present. The P&O algorithm directly controls the duty-cycle of the converter. As expected, the system response is poor and the P&O behavior is highly influenced by the dynamics of the converter. With lower sampling rate the system has an acceptable behavior and works almost well. In Figs. 15-16 one can notice that the input voltage of the converter has more ripple and the reference voltage determined by the P&O algorithm has an irregular behavior. In Figs. 17-18 one notices that the P&O algorithm gets totally confused when the sampling rate is increased and the system response is very poor. One can clearly notice that, for the same voltage increment and sampling rates, the performance of the MPPT P&O algorithm highly depends on the converter dynamics.

V. CONCLUSIONS

The results have demonstrated that the direct duty-cycle control is not recommended in this kind of application. First, one should not employ the MPPT algorithm as the controller of the converter because a simple PI compensator can achieve this task with low stead-state error and improved dynamic response. Second, the behavior of the MPPT algorithm highly depends on the converter dynamics. The algorithm senses the voltage and current of the PV array at every sampling interval and perturbs the reference (the voltage reference, in

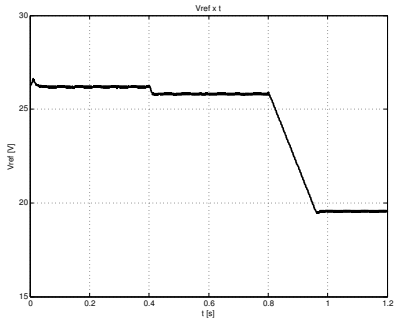

Figure 11. Reference voltage (V_{ref}) from the MPPT algorithm using PI compensator. ($T_s = 1\,\mathrm{ms}$, $\Delta_{\mathrm{V}} = 5\,\mathrm{mV}$)

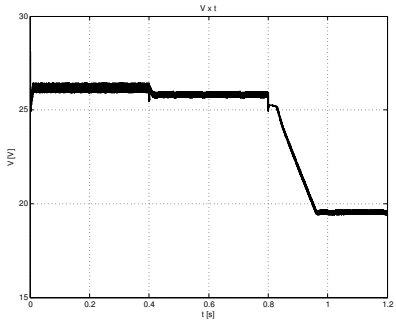

Figure 12. Input voltage of the converter (V) using PI compensator. ($T_s = 1\,\mathrm{ms}$, $\Delta_{\mathrm{V}} = 5\,\mathrm{mV}$)

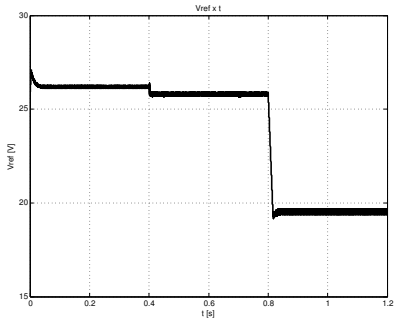

Figure 13. Reference voltage (V_{ref}) from the MPPT algorithm using PI compensator. ($T_s = 0.1\,\mathrm{ms}$, $\Delta_{\mathrm{V}} = 5\,\mathrm{mV}$)

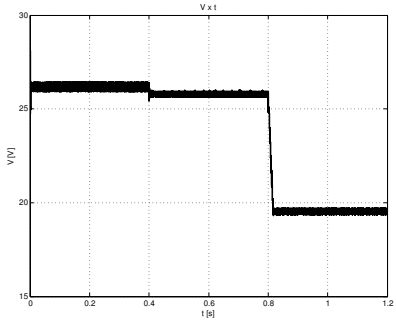

Figure 14. Input voltage (V) of the converter using PI compensator. ($T_s = 0.1\,\mathrm{ms}$, $\Delta_{\mathrm{V}} = 5\,\mathrm{mV}$)

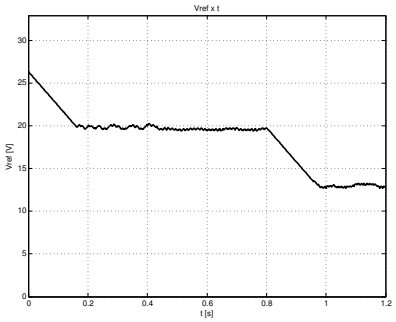

Figure 15. Reference voltage (V_{ref}) from the MPPT algorithm without PI compensator. ($T_s = 1\,\mathrm{ms}$, $\Delta_{\mathrm{V}} = 5\,\mathrm{mV}$)

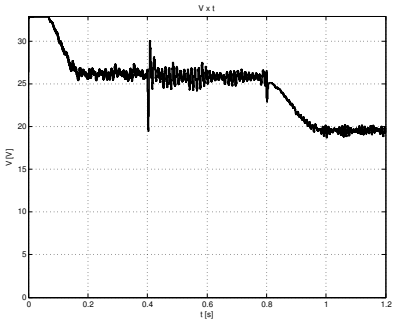

Figure 16. Input voltage (V) of the converter without PI compensator. ($T_s = 1\,\mathrm{ms}$, $\Delta_{\mathrm{V}} = 5\,\mathrm{mV}$)

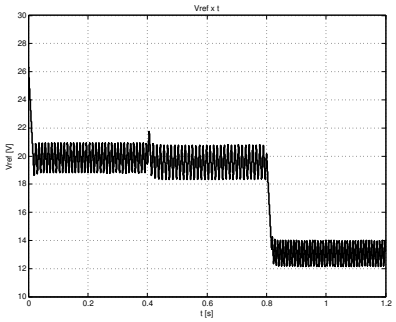

Figure 17. Reference voltage (V_{ref}) from the MPPT algorithm without PI compensator. ($T_s = 0.1\,\mathrm{ms}$, $\Delta_{\mathrm{V}} = 5\,\mathrm{mV}$)

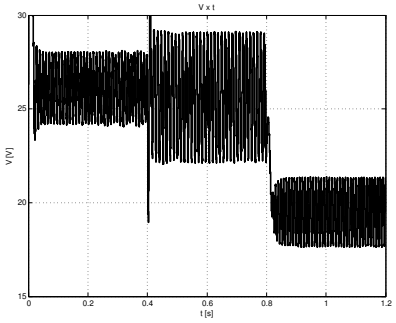

Figure 18. Input voltage (V) of the converter without PI compensator. ($T_s = 0.1\,\mathrm{ms}$, $\Delta_{\mathrm{V}} = 5\,\mathrm{mV}$)

this case) based on decisions of the algorithm. If the reference voltage is not properly followed by the converter the MPPT algorithm senses wrong current and voltage values and gets confused. In this paper the P&O algorithm has been employed but these conclusions are valid for other algorithms. By using the simplest MPPT algorithm, among other algorithms already presented in the literature [1], one concludes that even the simplest MPPT method can provide good results if the converter is controlled with a simple feedback controller with PI compensator.

ACKNOWLEDGMENT

REFERENCES

[1] M. C. Cavalcanti, K. C. Oliveira, G. M. S. Azevedo, and F. A. S. Neves. Comparative study of maximum power point tracking techniques for photovoltaic systems. *Brazilian Journal of Power Electronics, SOBRAEP*, 12(2):163–171, 2007.

[2] E. Koutroulis, K. Kalaitzakis, and N.C. Voulgaris. Development of a microcontroller-based, photovoltaic maximum power point tracking control system. *IEEE Transactions on Power Electronics*, 16(1):46–54, 2001.

[3] Chihchiang Hua, Jongrong Lin, and Chihming Shen. Implementation of a DSP-controlled photovoltaic system with peak power tracking. *IEEE Transactions on Industrial Electronics*, 45(1):99–107, 1998.

[4] N. Femia, G. Petrone, G. Spagnuolo, and M. Vitelli. Optimization of perturb and observe maximum power point tracking method. *IEEE Transactions on Power Electronics*, 20(4):963–973, 2005.

[5] N. Femia, G. Petrone, G. Spagnuolo, and M. Vitelli. Increasing the efficiency of P&O mppt by converter dynamic matching. In *IEEE International Symposium on Industrial Electronics*, p 1017–1021, vol. 2, 2004.

[6] N. Femia, G. Petrone, G. Spagnuolo, and M. Vitelli. Optimizing sampling rate of P&O mppt technique. In *IEEE PESC'04*, vol. 3, 2004.

[7] N. Femia, G. Petrone, G. Spagnuolo, and M. Vitelli. Optimizing duty-cycle perturbation of P&O mppt technique. In *IEEE PESC'04*, vol. 3, 2004.

[8] N. Femia, G. Petrone, G. Spagnuolo, and M. Vitelli. Perturb and observe mppt technique robustness improved. In *IEEE International Symposium on Industrial Electronics*, vol. 2, 2004.

[9] N. Femia, G. Petrone, G. Spagnuolo, and M. Vitelli. Increasing the efficiency of P&O mppt by converter dynamic matching. In *IEEE International Symposium on Industrial Electronics* , vol. 2, 2004.

[10] X. Liu and L.A.C. Lopes. An improved perturbation and observation maximum power point tracking algorithm for PV arrays. In *IEEE PESC'04*, vol. 3, 2004.

[11] A. S. Kislovski. Dynamic behavior of a constant-frequency buck converter power cell in a photovoltaic battery charger with a maximum power tracker. *5th Applied Power Electronics Conference and Exposition*, 1990.

[12] KC200GT high efficiency multicrystal photovoltaic module datasheet.

[13] M. G. Villalva, J. R. Gazoli, and E. Ruppert F. Comprehensive approach to modeling and simulation of photovoltaic arrays. *IEEE Transactions on Power Electronics*, vol. 25, no. 5, pp. 1198–1208, 2009.

[14] M. G. Villalva and E. Ruppert F. Buck converter with variable input voltage for photovoltaic applications. *Brazilian Power Electronics Conference, COBEP'07*, 2007.

[15] M. G. Villalva and E. Ruppert F. Dynamic analysis of the input-controlled buck converter fed by a photovoltaic array. *Revista Controle & Automação*, 19(4):463–474, 2008.

[16] M. G. Villalva and E. Ruppert F. Input-controlled buck converter for photovoltaic applications: modeling and design. *4th IET PEMD*, 2008.

[17] Robert W. Erickson and Dragan Maksimovic. *Fundamentals of Power Electronics*. Kluwer Academic Publishers, 2001.